IEEE Access
Multidisciplinary | Rapid Review | Open Access Journal

Received December 9, 2021, accepted December 18, 2021, date of publication December 22, 2021,
date of current version January 10, 2022.

Digital Object Identifier 10.1109/ACCESS.2021.3137639

Residual Error Feedback Zeroing Neural Network for Solving Time-Varying Sylvester Equation

KUNJIAN LI[1], CHENGZE JIANG[1], (Student Member, IEEE), XIUCHUN XIAO[1], HAOEN HUANG[1], YONGJIANG LI[2], AND JINGWEN YAN[3]

[1]School of Electronics and Information Engineering, Guangdong Ocean University, Zhanjiang 524088, China
[2]School of Mathematics and Computer, Guangdong Ocean University, Zhanjiang 524088, China
[3]College of Engineering, Shantou University, Shantou 515063, China

Corresponding author: Xiuchun Xiao (xcxiao@hotmail.com)

This work was supported in part by the Guangdong Basic and Applied Basic Research Foundation under grant 2021A1515011847, in part by the Special Project in Key Fields of Universities in Department of Education of Guangdong Province under grant 2019KZDZX1036, in part by the Guangdong Graduate Education Innovation Project, Graduate Summer School under grant 2020SQXX19, in part by the Guangdong Graduate Education Innovation Project, Graduate Academic Forum under Grant 202101, in part by the Key Lab of Digital Signal and Image Processing of Guangdong Province under Grant 2019GDDSIPL-01, in part by the Postgraduate Education Innovation Project of Guangdong Ocean University under Grant 202160, in part by the Innovative and Strong School Team Building Project under Grant 2017KCXTD015.

ABSTRACT In many fields, the issue of solving the time-varying Sylvester equation (TVSE) is commonly encountered. Consequently, finding its exact solution has become a research hotspot. In general, the ZNN and IEZNN models are the most useful algorithms that are frequently utilized to solve the TVSE problem. However, the ZNN model is borned with noise susceptibility and the IEZNN model loses the adaptive performance due to its constant coefficient in solving the TVSE problem. In this paper, a residual error feedback zeroing neural network (REFZNN) is proposed to adaptively solve the TVSE problem. The REFZNN model feeds back the residual error to the solustion system, which forms a feedback regulation to reduce the residual error between the system output and the system target. Then, the convergence and noise patience of the REFZNN model are proved by theoretical analyses. Finally, the validity of the proposed model is verified by designing computer simulation experiments and its superiority is confirmed by the performance comparisons with the ZNN and IEZNN models.

INDEX TERMS Time-varying problems, residual error, feedback, zeroing neural network (ZNN), Sylvester equation.

I. INTRODUCTION

Sylvester equation plays an important role in many fields, such as control system [1], [2], image processing [3], [4], and so on. In the recent decades, a lot of researches have been conducted on how to solve the Sylvester equation efficiently.

Originally, researchers studied many methods to solve the Sylvester equation [5], [6]. The most classical approach is Bartels-Stewart method. Only when the sampling period is large enough, Bartels-Stewart method and its extension are exploited to solve the time-invariant Sylvester equation by decomposing its coefficients into Schur and Hessenberg-Schur factorizations [7], [8]. However, Bartels-Stewart method holds the drawback of low efficiency and is unable to cope with time-varying Sylvester equation (TVSE).

The associate editor coordinating the review of this manuscript and approving it for publication was Rajeeb Dey.

In recent years, recurrent neural network (RNN) become quite prevalent owing to its parallel distribution and excellent properties [9]–[13]. Hence, it is applied in many fields such as robotics [14]–[16], signal processing [17], [18], and industrial applications [19]. Particularly, more and more researchers use it to solve Sylvester equation [20], [21]. The RNN model is divided into gradient neural network (GNN) model and zeroing neural network (ZNN) model [22]. On the one hand, as a classical neural network for solving algebraic problems, the GNN model has been widely used. Especially, the GNN model is employed to solve Sylvester equation by designing an error function that evolves along the direction of negative gradient. When the error function converges to zero, the solution of Sylvester equation can be obtained. Nevertheless, in order to predict the evolution direction of the solution model more accurately, the influence of time derivative information must be taken into account. Jin *et al.* indicated that

the GNN model cannot make good use of the time derivative information, which may cause the lag error that is not able to ignore when solving the TVSE problem [23]. Based on literature [23], Liao *et al.* modified the traditional GNN model and refined it into a form with adaptive coefficients to satisfy the requirement of solving the TVSE problem [24]. But this model cannot own noise patience in the process of solving the TVSE problem. Therefore, the above two methods fail to efficiently solve the TVSE problem.

On the other hand, Zhang *et al.* advised zeroing neural network (ZNN) model to solve the TVSE problem by using the derivative information of the error function of the objective equation [25]. On the basis of article [25], researchers modified the ZNN model to improve the convergence performance. For example, Li *et al.* designed a sign-bi-power activation function to accelerate the convergence process of ZNN model for solving the TVSE problem [26]. In addition, Shen *et al.* analyzed an effective time stability of ZNN model and defined an activation function to reduce the convergence time [27]. But these ZNN models have not any effective solution to deal with the noise interference encountered in the process of solving the TVSE problem. For the sake of noise patience, Jin *et al.* offered the integral-enhanced ZNN (IEZNN) model to reduce noise impressionability [28]. Besides, Zhang *et al.* provided a varying-parameter convergent-differential neural network (VP-CDNN), which has good stability in the process of solving the TVSE problem [29]. Unfortunately, these models do not make full use of the information of residual error. And there is not activation function in the evolution formula. In this paper, a residual error feedback zeroing neural network (REFZNN) model is proposed. This model combines the integral term and activation function to increase the noise patience. In addition, the feedback regulation of residual error is introduced into the REFZNN model for convergence capability.

The rest of this paper is divided into four parts. Firstly, we do some preparatory work and define REFZNN model in Section II. Then, the theoretical analyses are given to lay the foundation for the effectiveness of REFZNN model in Section III. Besides, the correctness of the theoretical analyses are verified by computer simulation experiments in Section IV, which confirms the advantages of REFZNN model. Finally, a summary is described in Section V. Before concluding this section, the highlights of this paper are listed as follows:

- A novel residual error feedback zeroing neural network (REFZNN) model is presented to effectively solve the TVSE problem.
- The theoretical analyses are given to ensure the convergence and noise patience of the REFZNN model.
- The advanced results of the REFZNN model for solving the TVSE problem are demonstrated by the comparisons with the ZNN and IEZNN models in the form of designed computer simulation experiments.

II. PROBLEM FORMULATION AND MODEL CONSTRUCTION

A. PROBLEM FORMULATION AND ZNN-TYPE SOLVERS

Typically, the TVSE problem can be characterized as follows:

$$A(t)X(t) - X(t)B(t) = -H(t), \tag{1}$$

where $A(t) \in \mathbb{R}^{m\times m}$, $B(t) \in \mathbb{R}^{n\times n}$, and $H(t) \in \mathbb{R}^{m\times n}$ represent known smoothly time-varying matrices. In addition, the matrix $X(t) \in \mathbb{R}^{m\times n}$ is the unknown matrix to be online solved. It's worth pointing that only the two eigenvalues of $A(t) \in \mathbb{R}^{m\times m}$ and $B(t) \in \mathbb{R}^{n\times n}$ are not equal at any moment, the TVSE problem (1) has a unique solution $X^*(t)$ [30]. The aim of this paper is to accurately solve the TVSE problem (1).

For supervising and tracking the solving process of the TVSE problem (1), the error function can be described as

$$E(t) = A(t)X(t) - X(t)B(t) + H(t) \in \mathbb{R}^{m\times n}. \tag{2}$$

Conforming to the Kronecker product definition, the following vectorization operation rule holds:

$$\mathrm{vec}(DCF) = \left(F^{\mathrm{T}} \otimes D\right) \mathrm{vec}(C)$$

where F, C, and D denote the general matrixes, the operator $\mathrm{vec}(\cdot)$ denotes the vectorization of a matrix, the symbol $\otimes$ represents Kronecker product operator, and the superscript ^{T} denotes the transpose of a matrix. Then, the error function (2) is vectorized as

$$\boldsymbol{e}(t) = N(t)\boldsymbol{x}(t) + \boldsymbol{h}(t), \tag{3}$$

where $\boldsymbol{e}(t) = \mathrm{vec}(E(t)) \in \mathbb{R}^{mn\times 1}$, $N(t) = I_n \otimes A(t) - B^{\mathrm{T}}(t) \otimes I_m \in \mathbb{R}^{mn\times mn}$, $\boldsymbol{x}(t) = \mathrm{vec}(X(t)) \in \mathbb{R}^{mn\times 1}$, $\boldsymbol{h}(t) = \mathrm{vec}(H(t)) \in \mathbb{R}^{mn\times 1}$. Besides, $I_m \in \mathbb{R}^{m\times m}$ and $I_n \in \mathbb{R}^{n\times n}$ denote the identity matries. According to previous researches, the evolution formula of the ZNN model is decipted as

$$\dot{\boldsymbol{e}}(t) = -\gamma\phi(\boldsymbol{e}(t)), \tag{4}$$

where the scale coefficient $\gamma > 0$ and $\phi(\cdot)$ represents an odd and monotonically increasing activation function. Specifically, the commonly utilized activiation functions are given:

1) POWER-SIGMOID ACTIVATION FUNCTION

$$\phi\left(e_j\right) = \begin{cases} \dfrac{1+\exp(-4)}{1-\exp(-4)}\dfrac{1-\exp\left(-4e_j\right)}{1+\exp\left(-4e_j\right)}, & \text{if } \left|e_j\right| < 1, \\ e_j^3, & \text{if } \left|e_j\right| \geq 1; \end{cases}$$

2) SIGN-BI-POWER ACTIVATION FUNCTION

$$\phi\left(e_j\right) = \frac{1}{2}\mathrm{Sig}^a\left(e_j\right) + \frac{1}{2}\mathrm{Sig}^{1/a}\left(e_j\right),$$

$$\mathrm{Sig}^a\left(e_j\right) = \begin{cases} \left|e_j\right|^a, & \text{if } e_j > 0, \\ 0, & \text{if } e_j = 0, \\ -\left|e_j\right|^a, & \text{if } e_j < 0; \end{cases}$$

where $a > 0$ and e_j represents the j-th subsystem of $\boldsymbol{e}(t)$.

Combining the equations (3) and (4), the ZNN model for solving the TVSE problem (1) is described as below:

$$N(t)\dot{\boldsymbol{x}}(t) = -\dot{N}(t)\boldsymbol{x}(t) - \dot{\boldsymbol{h}}(t) - \gamma\phi\big(N(t)\boldsymbol{x}(t) + \boldsymbol{h}(t)\big). \quad (5)$$

In order to achieve the performance of noise patience, an integration-enhanced ZNN (IEZNN) model is desiged:

$$\dot{\boldsymbol{e}}(t) = -\gamma\phi\big(\boldsymbol{e}(t)\big) - \mu\int_0^t \boldsymbol{e}(\tau)\mathrm{d}\tau, \quad (6)$$

where the parameter $\mu > 0$ is utilized to control the influence of the integration item $\int_0^t \boldsymbol{e}(\tau)\mathrm{d}\tau$. Inserting (3) into (6), the IEZNN model to solve the TVSE problem (1) can be arranged as

$$\begin{aligned} N(t)\dot{\boldsymbol{x}}(t) = & -\dot{N}(t)\boldsymbol{x}(t) - \dot{\boldsymbol{h}}(t) \\ & -\gamma\phi\big(N(t)\boldsymbol{x}(t) + \boldsymbol{h}(t)\big) \\ & -\mu\int_0^t \big(N(\tau)\boldsymbol{x}(\tau) + \boldsymbol{h}(\tau)\big)\mathrm{d}\tau. \end{aligned} \quad (7)$$

B. REFZNN MODEL CONSTRUCTION

In order to solve TVSE problem (1) more advantageously, a residual error feedback zeroing neural network (REFZNN) model is proposed as follows:

$$\begin{aligned} \dot{\boldsymbol{e}}(t) = & -\lambda\big(\boldsymbol{e}(t)\big)\phi\big(\boldsymbol{e}(t)\big) \\ & -\mu\phi\bigg(\boldsymbol{e}(t) + \int_0^t \lambda\big(\boldsymbol{e}(\tau)\big)\phi\big(\boldsymbol{e}(\tau)\big)\mathrm{d}\tau\bigg). \end{aligned} \quad (8)$$

Here, the time-varying adaptive coefficient $\lambda\big(\boldsymbol{e}(t)\big)$ is based on the residual error of the solution system can be constructed as

- exponential adaptive coefficient

$$\lambda\big(\boldsymbol{e}(t)\big) = b^{\|\boldsymbol{e}(t)\|_2} + b \cdot \exp(\|\boldsymbol{e}(t)\|_2 + b);$$

- absolute value adaptive coefficient

$$\lambda\big(\boldsymbol{e}(t)\big) = b\,|\log_2(\|\boldsymbol{e}(t)\|_2)| + b;$$

- fraction adaptive coefficient

$$\lambda\big(\boldsymbol{e}(t)\big) = \frac{b\log_2(\|\boldsymbol{e}(t)\|_2)}{\log_{10}(\|\boldsymbol{e}(t)\|_2)};$$

where the parameter $b > 1$. Besides, the signs $\|\cdot\|_2$ and $|\cdot|$ represent the second norm of a matrix and the absolute value of a number, respectively.

Consequently, fusing equations (3) and (8), the REFZNN model for solving the TVSE problem (1) can be denoted:

$$\begin{aligned} N(t)\dot{\boldsymbol{x}}(t) = & -\dot{N}(t)\boldsymbol{x}(t) - \dot{\boldsymbol{h}}(t) \\ & -\lambda\big(\boldsymbol{e}(t)\big)\phi\big(N(t)\boldsymbol{x}(t) + \boldsymbol{h}(t)\big) \\ & -\mu\phi\bigg(N(t)\boldsymbol{x}(t) + \boldsymbol{h}(t) \\ & + \int_0^t \lambda\big(\boldsymbol{e}(\tau)\big)\phi\big(N(\tau)\boldsymbol{x}(\tau) + \boldsymbol{h}(\tau)\big)\mathrm{d}\tau\bigg). \end{aligned} \quad (9)$$

III. THEORETICAL ANALYSES

In this section, the theoretical analyses of the convergence and robustness of REFZNN model (8) are depicted in details.

A. CONVERGENCE ANALYSES

In this subsection, The convergence of REFZNN model (8) is validated as the following theorem.

Theorem 1: The computational solution solved by REFZNN model (8) is globally close to the theoretical solution of the TVSE problem (1).

Proof: As defined in the previous section, $e_j(t)$ is regarded as the j-th subsystem of $\boldsymbol{e}(t)$, where $j \in 1, 2, \ldots, mn$. Then, we can obtain the following formula:

$$\begin{aligned} \dot{e}_j(t) = & -\lambda\big(e_j(t)\big)\phi\big(e_j(t)\big) \\ & -\mu\phi\bigg(e_j(t) + \int_0^t \lambda\big(e_j(\tau)\big)\phi\big(e_j(\tau)\big)\mathrm{d}\tau\bigg). \end{aligned} \quad (10)$$

To simplify writing, we define the following expression as

$$q_j(t) = e_j(t) + \int_0^t \lambda\big(e_j(\tau)\big)\phi\big(e_j(\tau)\big)\mathrm{d}\tau. \quad (11)$$

Consequently, the time derivative of $q_j(t)$ can comfortably be obtained as

$$\dot{q}_j(t) = \dot{e}_j(t) + \lambda\big(e_j(t)\big)\phi\big(e_j(t)\big). \quad (12)$$

Linking equations (10), (11), and (12), it is clear that the following equation can be achieved as

$$\dot{q}_j(t) = -\mu\phi\big(q_j(t)\big). \quad (13)$$

The above formula is consistent with the ZNN model (4). According to [31], $q_j(t)$ will globally converge to zero.

Furthermore, the Lyapunov candidate function in [32], [33] can be created as follows:

$$G_j(t) = \frac{1}{2}\kappa e_j^2(t) + \frac{1}{2}q_j^2(t), \quad (14)$$

where $\kappa > 0$. Undoubtedly, $G_j(t)$ is a positive definite function owing to $G_j(t) > 0$ for $e_j(t) \neq 0$ or $q_j(t) \neq 0$ as well as $G_j(t) = 0$ for $e_j(t) = q_j(t) = 0$.

At first, we define $G_0 = G_j(0) = \frac{1}{2}\kappa e_j^2(0) + \frac{1}{2}q_j^2(0)$, where $e_j(0)$ and $q_j(0)$ are random initial values of $e_j(t)$ and $q_j(t)$. After, the time derivative of $G_j(t)$ can be easily gained as

$$\begin{aligned} \dot{G}_j(t) &= \kappa e_j(t)\dot{e}_j(t) + q_j(t)\dot{q}_j(t) \\ &= -\kappa\mu e_j(t)\phi\big(q_j(t)\big) - \kappa\lambda\big(e_j(t)\big)e_j(t)\phi\big(e_j(t)\big) \\ &\quad -\mu q_j(t)\phi\big(q_j(t)\big). \end{aligned} \quad (15)$$

Then, assume that there exists a moment where $G_j(t)$ satisfies $G_j(t) \leq G_0$, the following inequalities can be obtained as

$$\frac{1}{2}\kappa e_j^2(t) \leq G_0, \ \frac{1}{2}q_j^2(t) \leq G_0.$$

It is easy to get as follows:

$$|e_j(t)| \leq \sqrt{2G_0/\kappa}, \quad |q_j(t)| \leq \sqrt{2G_0}.$$

According to differential mean-value theorem, it can be acquired:

$$\frac{\phi\left(q_j(t)\right) - \phi(0)}{q_j(t) - 0} = \left.\frac{\partial\phi\left(q_j(\delta)\right)}{\partial q_j}\right|_{q_j(\delta)\in\Upsilon_1}, \quad (16)$$

where the set Υ_1 denotes an interval that satisfies $\Upsilon_1 = \left\{q_j(t) \in \mathbb{R}, \left|q_j(t)\right| \leqslant \sqrt{2G_0}\right\}$. Since $\phi(\cdot)$ is odd monotonic increasing function, $\partial\phi\left(q_j(\delta)\right)/\partial q_j > 0$ holds true. We presume that $S_1 = \max\left\{\partial\phi\left(q_j(t)\right)/\partial q_j\right\}\big|_{q_j(t)\in\Upsilon_1} > 0$, and the inequality holds:

$$\left|\phi\left(q_j(t)\right)\right| \leqslant S_1\left|q_j(t)\right|. \tag{17}$$

Based on (17), it can be facilely gained as

$$\left|e_j(t)\phi\left(q_j(t)\right)\right| \leqslant S_1\left|e_j(t)\right|\cdot\left|q_j(t)\right|. \tag{18}$$

Similarly, S_2, S_3 can be generated as

$$\begin{aligned} S_2 &= \min\left\{\partial\phi\left(e_j(t)\right)/\partial e_j\right\}\big|_{e_j(t)\in\Upsilon_2} > 0,\\ S_3 &= \min\left\{\partial\phi\left(q_j(t)\right)/\partial q_j\right\}\big|_{q_j(t)\in\Upsilon_1} > 0, \end{aligned}$$

where the set $\Upsilon_2 = \left\{e_j(t) \in R, \left|e_j(t)\right| \leqslant \sqrt{2G_0/\kappa}\right\}$ is a closed interval. Correspondingly, the following inequalities can be acquired:

$$\left|\phi\left(e_j(t)\right)\right| \geqslant S_2\left|e_j(t)\right|, \left|\phi\left(q_j(t)\right)\right| \geqslant S_3\left|q_j(t)\right|. \tag{19}$$

Combining equations (15), (18), and (19), the inequality can be delivered:

$$\begin{aligned} \dot{G}_j(t) &= -\kappa\mu e_j(t)\phi\big(q_j(t)\big) - \kappa\lambda\big(e_j(t)\big)e_j(t)\phi\big(e_j(t)\big)\\ &\quad -\mu q_j(t)\phi\big(q_j(t)\big)\\ &\leqslant \kappa\mu\left|e_j(t)\phi\left(q_j(t)\right)\right| - \kappa\lambda\big(e_j(t)\big)e_j(t)\phi\left(e_j(t)\right)\\ &\quad -\mu q_j(t)\phi\left(q_j(t)\right)\\ &\leqslant \kappa\mu S_1\left|e_j(t)\right|\cdot\left|q_j(t)\right| - \kappa\lambda\big(e_j(t)\big)S_2e_j^2(t)\\ &\quad -\mu S_3q_j^2(t)\\ &= -\kappa\left(\frac{2\lambda\big(e_j(t)\big)S_2e_j(t) - \mu S_1\left|q_j(t)\right|}{2\sqrt{\lambda\big(e_j(t)\big)S_2}}\right)^2\\ &\quad -\kappa\left(\frac{\mu S_3}{\kappa} - \frac{\mu^2S_1^2}{4\lambda\big(e_j(t)\big)S_2}\right)q_j^2(t). \end{aligned} \tag{20}$$

Evidently, when $G_j(t) \leq G_0$, the premise of $\dot{G}_j(t) \leq 0$ is

$$\frac{\mu S_3}{\kappa} - \frac{\mu^2S_1^2}{4\lambda\big(e_j(t)\big)S_2} \geq 0, \tag{21}$$

according to the inequality (21) and $\kappa > 0$, κ is keep in $(0, 4\lambda(e_j(t))S_2S_3/\mu S_1^2]$. Therefore, it is available to find a qualified κ that makes $G_j(t) \leq G_0$ always hold true for any time t. In other words, $\dot{G}_j(t) \leq 0$ maintains correctness for all time. Moreover, $\dot{G}_j(t)$ is equivalent with zero only when $e_j(t) = q_j(t) = 0$. That is to say, the computational solution of REFZNN model (8) can globally converge to the theoretical solution of the TVSE problem (1).

The proof is thus completed. ■

B. ROBUSTNESS ANALYSES

The robustness of REFZNN model (8) disturbed by various noises will be verified with two theorems in this part.

Theorem 2: Under the perturbation of constant noise $\zeta(t) = \bar{\zeta}$, the residual error $\|\boldsymbol{e}(t)\|_2$ of the proposed REFZNN model (8) to solve the TVSE problem (1) globally converges to zero along with the evolution direction.

Proof: We define $\bar{\zeta}_j$ the j-th subelement of $\bar{\zeta}$, and the j-th subsystem of equation (8) can be expressed to

$$\begin{aligned} \dot{e}_j(t) &= -\lambda\big(e_j(t)\big)\phi\big(e_j(t)\big)\\ &\quad -\mu\phi\left(e_j(t) + \int_0^t\lambda\big(e_j(\tau)\big)\phi\big(e_j(\tau)\big)\mathrm{d}\tau\right) + \bar{\zeta}_j\\ &= -\lambda\big(e_j(t)\big)\phi\big(e_j(t)\big) - \mu\phi\big(q_j(t)\big) + \bar{\zeta}_j. \end{aligned} \tag{22}$$

Then, combining with equation (13), it is earned:

$$\dot{q}_j(t) = -\mu\phi\big(q_j(t)\big) + \bar{\zeta}_j. \tag{23}$$

The Lyapunov candidate function is formed as follows:

$$L_j(t) = \frac{1}{2}\left(\mu\phi\big(q_j(t)\big) - \bar{\zeta}_j\right)^2. \tag{24}$$

Apparently, $L_j(t)$ is positive definite. Its derivative about time t can be written as

$$\begin{aligned} \dot{L}_j(t) &= \mu\left(\mu\phi\left(q_j(t)\right) - \bar{\zeta}_j\right)\frac{\partial\phi\left(q_j(t)\right)}{\partial q_j}\dot{q}_j(t)\\ &= -\mu\frac{\partial\phi\left(q_j(t)\right)}{\partial q_j}\left(\mu\phi\left(q_j(t)\right) - \bar{\zeta}_j\right)^2. \end{aligned} \tag{25}$$

In line with the above analyses, it is effortless to realize that $\dot{L}_j(t)$ is negative definite. Namely, $\lim_{t\to+\infty}L_j(t) = 0$ as well as $\lim_{t\to+\infty} -\mu\phi\left(q_j(t)\right) + \bar{\zeta}_j = 0$. Therefore, $\lim_{t\to+\infty}\dot{e}_j(t) = -\lambda\big(e_j(t)\big)\phi\big(e_j(t)\big)$ is established, which is consistent with the ZNN model (4). That is to say, $e_j(t)$ can convergent to zero. The proof is thus completed. ■

Theorem 3: Under the perturbation of linear noise $\zeta(t) = \zeta t$, the upper bound of the residual error $\|\boldsymbol{e}(t)\|_2$ of the proposed REFZNN model (8) for solving the TVSE problem (1) is $n\left|\dot{\zeta}_{\max}(t)\right| \Big/ \xi_{\min}\mu\lambda_{\min}\big(e_j(t)\big)$ when $t \to +\infty$. Besides, $\lambda_{\min}\big(e_j(t)\big)$ is the minimum of $\lambda\big(e_j(t)\big)$, $\xi_j = \left|\phi\left(e_j(t)\right)\right|/\left|e_j(t)\right| \geqslant 1$ and $\xi = \min\left\{\xi_j \mid j \in 1, 2, \ldots, mn\right\}$. In addition, $\zeta_j(t)$ is the j-th subsystem of $\zeta(t)$, $\left|\dot{\zeta}_{\max}(t)\right|$ is the upper bound of $\left|\dot{\zeta}_j(t)\right|$.

Proof: Similar to the proof of Theorem 2, the following dynamics can be acquired as

$$\dot{q}_j(t) = -\mu\phi\big(q_j(t)\big) + \zeta_j(t). \tag{26}$$

Then, an auxiliary function is designed as $u_j(t) = q_j^2(t)/2$ and the time derivative of $u_j(t)$ can be procured:

$$\begin{aligned} \dot{u}_j(t) &= \left(-\mu\phi\left(q_j(t)\right) + \zeta_j(t)\right)q_j(t)\\ &= -\mu q_j(t)\phi\left(q_j(t)\right) + \zeta_j(t)q_j(t). \end{aligned} \tag{27}$$

Obviously, $-\mu q_j(t)\phi\big(q_j(t)\big) \leq 0$ is always true. Because $\zeta_j(t)q_j(t) \leq 0$ is a sufficient and non-essential condition for $\dot{u}_j(t) \leq 0$, the following discussion focuses on $\zeta_j(t)q_j(t) > 0$.

In case of $\zeta_j(t)q_j(t) > 0$, $u_j(t)$ may increase. On the one hand, $|q_j(t)| = \sqrt{u_j(t)}$ will also increase with the increase of $u_j(t)$. On the other hand, $|-\mu\phi(q_j(t)) + \zeta_j(t)|$ will decrease along with the increasement of $|q_j(t)|$, which do not stop until $(-\mu\phi(q_j(t)) + \zeta_j(t)) = 0$. This makes $\dot{u}_j(t) = 0$ with $u_j(t)$ getting the maximum. Therefore, it manifests that $|q_j(t)|$ satisfies the following inequality:

$$|q_j(t)| \leqslant \left|\phi^{-1}\left(\zeta_j(t)/\mu\right)\right|,$$

where $\phi^{-1}(\cdot)$ denotes the inverse function of $\phi(\cdot)$. Because $|\phi(\cdot)| \geq |\phi_{\text{lin}}(\cdot)|$, $\phi^{-1}(\cdot) \leq |\phi_{\text{lin}}(\cdot)|$, where $\phi_{\text{lin}}(\cdot)$ represents linear activation function, and its definition as follows:

$$\phi\left(e_j\right) = e_j,$$

the above inequality can be rewiritten as

$$-\left|\zeta_j(t)/\mu\right| \leqslant q_j(t) \leqslant \left|\zeta_j(t)/\mu\right|.$$

For an arbitrary moment $t_1 > 0$, it satisfies $Q_1 = e_j(t_1) + \int_0^{t_1} \lambda(e_j(\tau))\phi\left(e_j(\tau)\right) \mathrm{d}\tau$. Similarly, t_2 corresponds to $Q_2 = e_j(t_2) + \int_0^{t_2} \lambda(e_j(\tau))\phi\left(e_j(\tau)\right) \mathrm{d}\tau$.

Assuming $\lambda(e_j(t))\phi\left(e_j(t)\right) > \left|\dot{\zeta}_j(t)/\mu\right|$ in $[t_1, t_2]$ with $t_2 - t_1 = \delta$, it generates the following relationship expression:

$$\begin{aligned}
&Q_2 - Q_1 \\
&= \left(e_j(t_2) - e_j(t_1)\right) + \int_0^{t_2} \lambda(e_j(\tau))\phi\left(e_j(\tau)\right) \mathrm{d}\tau \\
&\quad - \int_0^{t_1} \lambda(e_j(\tau))\phi\left(e_j(\tau)\right) \mathrm{d}\tau \\
&= \left(e_j(t_1+\delta) - e_j(t_1)\right) + \int_{t_1}^{t_1+\delta} \lambda(e_j(\tau))\phi\left(e_j(\tau)\right) \mathrm{d}\tau \\
&\geqslant \int_{t_1}^{t_1+\delta} \lambda(e_j(\tau))\phi\left(e_j(\tau)\right) \mathrm{d}\tau - e_j(t_1). \qquad (28)
\end{aligned}$$

According to the above analyses, the inequality is obtained as

$$\begin{aligned}
&\left|\zeta_j(t_1+\delta)/\mu\right| - Q_1 \\
&\leqslant \left|\zeta_j(t_1)/\mu\right| + \left|\zeta_j(t_1+\delta)/\mu - \zeta_j(t_1)/\mu\right| - Q_1 \\
&= \left|\zeta_j(t_1)/\mu\right| + \left|\int_{t_1}^{t_1+\delta} \left(\dot{\zeta}_j(\tau)/\mu\right) \mathrm{d}\tau\right| - Q_1 \\
&\leqslant \left|\zeta_j(t_1)/\mu\right| + \int_{t_1}^{t_1+\delta} \left|\dot{\zeta}_j(\tau)/\mu\right| \mathrm{d}\tau - Q_1. \qquad (29)
\end{aligned}$$

Combing equations (28) and (29), it can be getted:

$$\begin{aligned}
&Q_2 - \left|\zeta_j(t_1+\delta)/\mu\right| \\
&\quad \geqslant \int_{t_1}^{t_1+\delta} \left(\lambda(e_j(\tau))\phi\left(e_j(\tau)\right) - \left|\dot{\zeta}_j(\tau)/\mu\right|\right) \mathrm{d}\tau \\
&\qquad - \left(\left|\zeta_j(t_1)/\mu\right| + e_j(t_1) + Q_1\right). \qquad (30)
\end{aligned}$$

Due to $\lambda(e_j(t))\phi\left(e_j(t)\right) - \left|\dot{\delta}_j(t)/\mu\right| > 0$ and $Q_2 \leq \left|\zeta_j(t_1+\delta)/\mu\right|$, it can be acquired as

$$\begin{aligned}
&\int_{t_1}^{t_1+\delta} \left(\lambda(e_j(\tau))\phi\left(e_j(\tau)\right) - \left|\dot{\zeta}_j(\tau)/\mu\right|\right) \mathrm{d}\tau \\
&\qquad \leqslant \left|\zeta_j(t_1)/\mu\right| + e_j(t_1) + Q_1. \qquad (31)
\end{aligned}$$

It must be emphasized that the left side of equation (31) is a increasing function about δ, while the right side of equation (31) is a fixed value. Therefore, it is easily to attain that $\lim_{t\to+\infty} \lambda(e_j(t))\phi\left(e_j(t)\right) - \left|\dot{\zeta}_i(t)/\mu\right| = 0$.

Assuming $\lambda(e_j(t))\phi\left(e_j(t)\right) < \dot{\zeta}_j(t_1)/\mu < 0$, we can similarly earn that $\lim_{t\to+\infty} \lambda(e_j(t))\phi\left(e_j(t)\right) + \left|\dot{\zeta}_i(t)/\mu\right| = 0$.

To sum up, it can be decured that $\lambda(e_j(t))\phi\left(e_j(t)\right) \in \left[-\left|\dot{\zeta}_j(t)\right|/\mu, \left|\dot{\zeta}_j(t)\right|/\mu\right]$. Furthermore, this shows $e_j(t)$ converges to $\left[-\left|\dot{\zeta}_j(t)\right|/\mu\xi_j\lambda(e_j(t)), \left|\dot{\zeta}_j(t)\right|/\mu\xi_j\lambda(e_j(t))\right]$. So $\|\mathbf{e}(t)\|_2$ satisfies:

$$0 \leqslant \|\mathbf{e}(t)\|_2 = \sqrt{\sum_{i=1}^{n^2} e_j^2(t)} \leqslant n\left|e_{\max}(t)\right|, \qquad (32)$$

where $|e_{\max}(t)|$ denotes the largest value among $\left|e_j(t)\right|, \forall i \in \left\{1, 2, \ldots, n^2\right\}$. Finally, we can conclude that the residual error $\|\mathbf{e}(t)\|_2$ of the REFZNN model (8) disturbed by linear noise converges to the interval $\left[0, n\left|\dot{\zeta}_{\max}(t)\right|/\xi\mu\lambda_{\min}(e_j(t))\right]$.

The proof is thus completed. ■

IV. EXPERIMENTAL VERIFICATION

The previous section has theoretically analyzed the convergence and robust performance of the proposed REFZNN model (8). In this section, the above theoretical results will be confirmed through computer simulation experiments. The following time-varying matrices are applied as an example of the corresponding matrices in TVSE problem (1) for simulation experiments as below.

$$\begin{cases}
A(t) = \begin{bmatrix} \sin(t) & \cos(t) \\ -\cos(t) & \sin(t) \end{bmatrix}, \\
B(t) = \begin{bmatrix} 0.1\sin(t) & 0 \\ 0 & 0.2\cos(t) \end{bmatrix}, \\
H(t) = \begin{bmatrix} 0.1\sin^2(t) - 1 & -0.2\cos^2(t) \\ 0.1\sin(t)\ \cos(t) & 0.2\sin(t)\ \cos(t) - 1 \end{bmatrix}.
\end{cases}$$

Then, the corresponding time-varying matrices $N(t)$, and time-varying vector $\boldsymbol{h}(t)$ in the equation (3) can be written as

$$\begin{cases}
N(t) = \left(\begin{bmatrix} 1 & 0 \\ 0 & 1 \end{bmatrix} \otimes \begin{bmatrix} \sin(t) & \cos(t) \\ -\cos(t) & \sin(t) \end{bmatrix}\right. \\
\quad \left. - \begin{bmatrix} 0.1\sin(t) & 0 \\ 0 & 0.2\cos(t) \end{bmatrix} \otimes \begin{bmatrix} 1 & 0 \\ 0 & 1 \end{bmatrix}\right), \\
\boldsymbol{h}(t) = \begin{bmatrix} 0.1\sin^2(t) - 1 \\ 0.1\sin(t)\ \cos(t) \\ -0.2\cos^2(t) \\ 0.2\sin(t)\ \cos(t) - 1 \end{bmatrix}.
\end{cases}$$

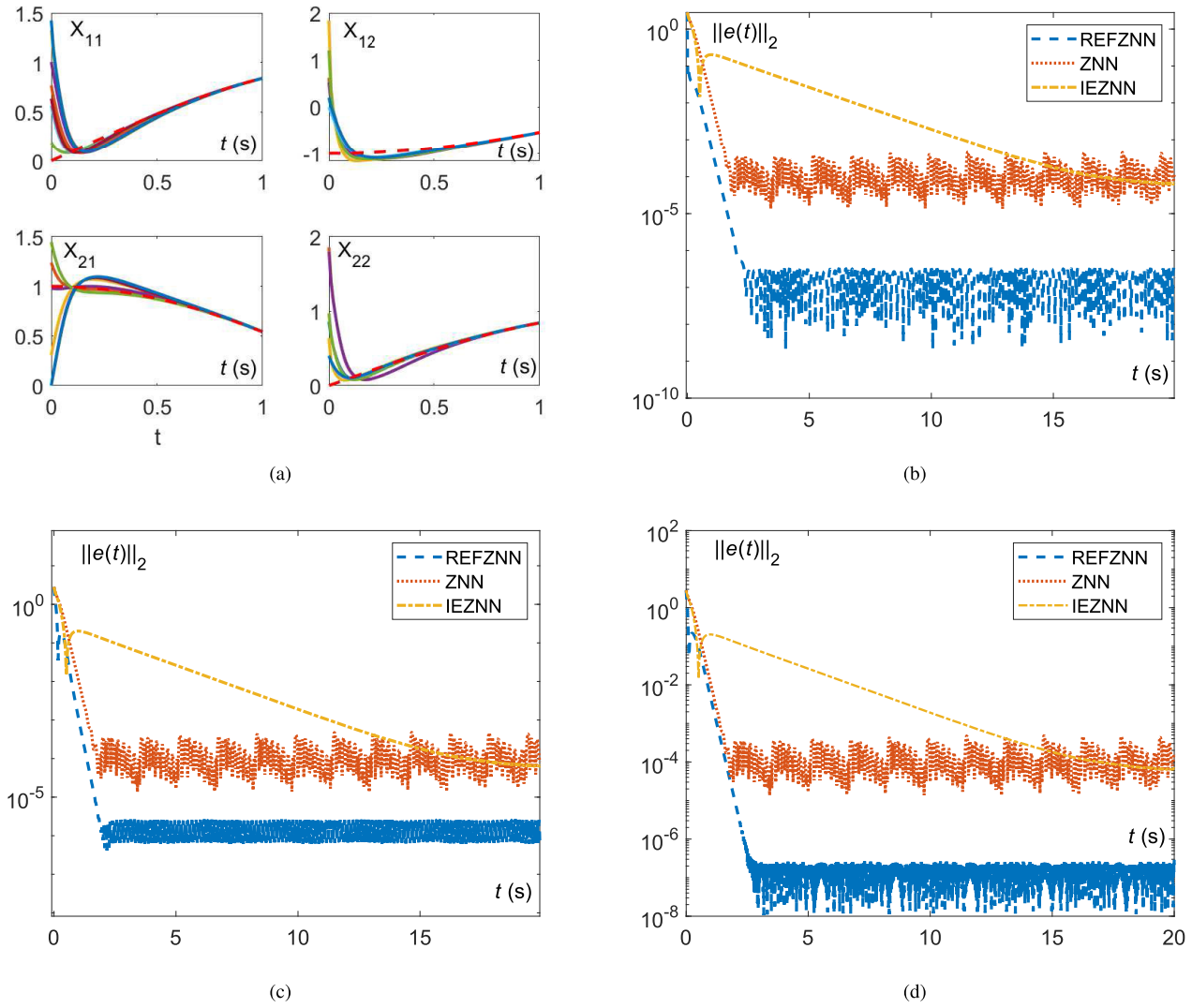

FIGURE 1. The experimental results of REFZNN model (8) in the case of noise-free, where $\mu = b = 3$. (a) The convergence process of the calculation synthesized by REFZNN model (8). (b) The residual errors $\|e(t)\|_2$ of ZNN model (4), IEZNN model (6), and REFZNN model (8) using exponential adaptive coefficient under zero noise. (c) The residual errors $\|e(t)\|_2$ of ZNN model (4), IEZNN model (6), and REFZNN model (8) using absolute value adaptive coefficient under zero noise. (d) The residual errors $\|e(t)\|_2$ of ZNN model (4), IEZNN model (6), and REFZNN model (8) using fraction adaptive coefficient under zero noise.

A. EXPERIMENTAL RESULTS OF NOISE-FREE CASE

In the case of noise-free, the experimental results of the REFZNN model (8) for solving the TVSE problem (1) are exhibited in Fig. 1. As shown in Fig. 1 (a), the red dotted line denotes the theoretical solution of the TVSE problem (1), and the other solid lines with different colors represent the calculated solutions tallied by the REFZNN model (8) with $\mu = b = 3$ from eight different initial values. Clearly, from eight arbitrary initial points, the computational solutions of the REFZNN model (8) can converge to the theoretical solution of the TVSE problem (1) in a very short time. Specifically, it converges to the theoretical solution within 1 s. Thus, the correctness of Theorem 1 is well verified.

As shown in Figs. 1 (b)–(d), they respectively represent the residual errors of the REFZNN model (8) composed of exponential, absolute, and fractional adaptive coefficients to solve the TVSE problem (1). Clearly, no matter which adaptive coefficient is used, the residual errors of REFZNN model (8) can converge to of order 10^{-6}. However, those of ZNN model (4) only converges of order 10^{-4} and IEZNN model (6) does not converge in t = 20 s. The advantage of REFZNN model (8) to solve the TVSE problem (1) is presented.

B. EXPERIMENTAL RESULTS OF VARIOUS NOISES

The following two cases are considered for computer simulation experiments to verify the robustness of the REFZNN model (8).

1) Constant noise: In this part, the simulation results of ZNN model (4), IEZNN model (6), and REFZNN model (8)

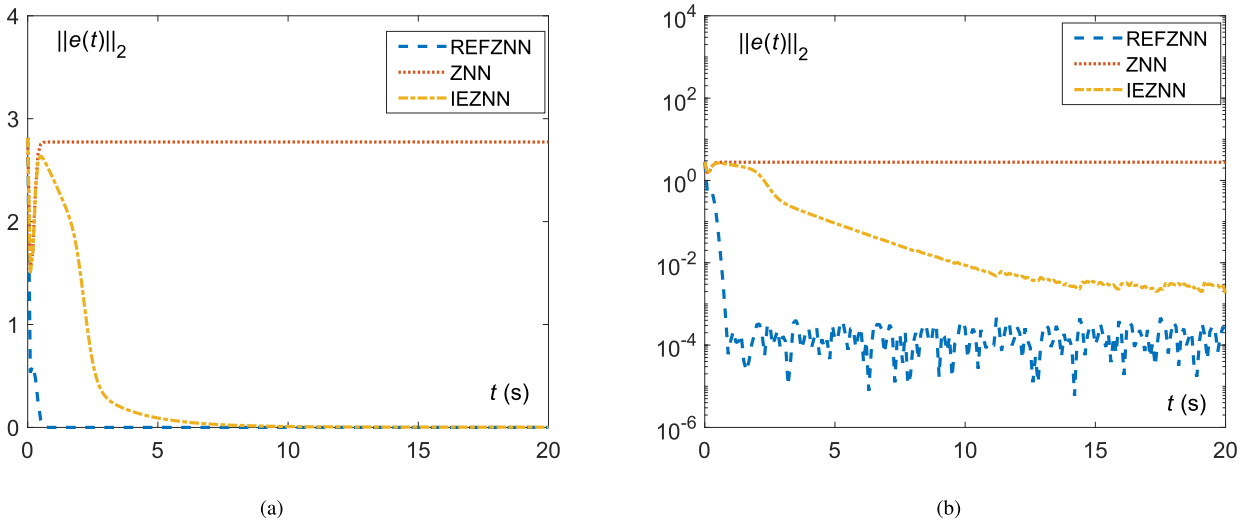

FIGURE 2. The residual error $\|e(t)\|_2$ of ZNN model (4), IEZNN model (6), and REFZNN model (8) under constant noise interference, where $\mu = b = 3$. (a)Linear residual error diagram of ZNN model (4), IEZNN model (6), and REFZNN model (8) in the case of constant noise $\zeta(t) = \bar{\zeta} = [8]^4$. (b)Log residual error diagram of ZNN model (4), IEZNN model (6), and REFZNN model (8) in the case of constant noise $\zeta(t) = \bar{\zeta} = [8]^4$.

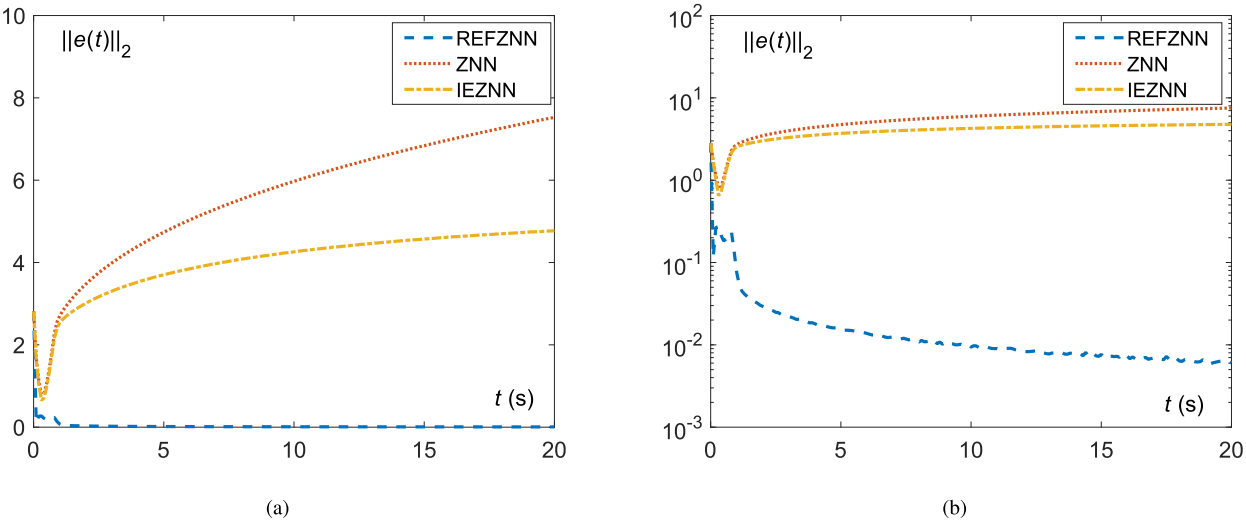

FIGURE 3. The residual error $\|e(t)\|_2$ of ZNN model (4), IEZNN model (6), and REFZNN model (8) under linear noise interference, where $\mu = b = 3$. (a)Linear residual error diagram of ZNN model (4), IEZNN model (6), and REFZNN model (8) in the case of linear noise $\zeta(t) = \zeta t = [8t]^4$. (b)Log residual error diagram of ZNN model (4), IEZNN model (6), and REFZNN model (8) in the case of linear noise $\zeta(t) = \zeta t = [8t]^4$.

under constant noise are demonstrated in Fig. 2. For illustration and comparison, every value of constant noise is set to 8. The values of μ and b are both taken as 3. It is reflected from Figs. 2 (a) that the residual error of the REFZNN model (8) can immediately converge to an accuracy close to zero. For a clearer presentation, a comparative log plot of the residual errors of the three models is furnished in Figs. 2 (b). As exhibited in Figs. 2 (b), starting from any initial value, the residual error of the REFZNN model (8) under constant noise reduces to of order 10^{-4} within 1 s. So that the correctness of Theorem 2 is proved. In contrast, the residual errors of the IEZNN model (6) and ZNN model (4) remain a high level for a long time in the same condition. Specifically, the residual error of the ZNN model (4) converges to of order 10^0, and the residual error of the IEZNN model (6) decreases to of order 10^{-3}.

2) Linear noise: For the authenticity and effectiveness of the experiment, we set the value of linear noise as $8t$, and the values of μ and b are both 3. Similarly, as visualized in Figs. 3 (a)–(b), starting from an arbitrary initial value, the residual error of the REFZNN model (8) minimizes to of order 10^{-2} within 1 s under the interference of linear noise. However, the ZNN model (4) and IEZNN model (6) keep an upward trend. It can be seen from the experimental results that

the residual errors of ZNN model (4) and IEZNN model (6) are 100 times of those of the REFZNN model (8) in t = 20 s. As a result, the rightness of Theorem 3 is approved, and the superiority of REFZNN model (8) is further demonstrated.

V. CONCLUSION AND FUTURE WORK

In this paper, a residual error feedback neural network (REFZNN) model for solving the TVSE problem (1) is proposed for the first time. Compared with the ZNN model (4) and IEZNN model (6), the REFZNN model (8) has residual error feedback adjustment mechanism, which can make the system more stable. The convergence and robustness of the REFZNN model (8) to solve the target problems are analyzed theoretically. At the same time, the simulation results suggest that the REFZNN model (8) possesses superiority in convergence speed and solution accuracy under different residual error feedback functions. In addition, the simulation results also verify the stability of the REFZNN model (8) in solving the TVSE problem (1) under the influence of different noises. In general, the advantages of REFZNN model are highlighted. On top of that, the focus of future work is to use the REFZNN model to solve other problems.

REFERENCES

[1] V. L. Syrmos and F. L. Lewis, "Output feedback eigenstructure assignment using two Sylvester equations," *IEEE Trans. Autom. Control*, vol. 38, no. 3, pp. 495–499, Mar. 1993.

[2] V. L. Syrmos, "Disturbance decoupling using constrained Sylvester equations," *IEEE Trans. Autom. Control*, vol. 39, no. 4, pp. 797–803, Apr. 1994.

[3] Q. Wei, N. Dobigeon, and J. Tourneret, "Fast fusion of multi-band images based on solving a Sylvester equation," *IEEE Trans. Image Process.*, vol. 24, no. 11, pp. 4109–4121, Nov. 2015.

[4] Q. Wei, N. Dobigeon, J.-Y. Tourneret, J. Bioucas-Dias, and S. Godsill, "R-FUSE: Robust fast fusion of multiband images based on solving a Sylvester equation," *IEEE Signal Process. Lett.*, vol. 23, no. 11, pp. 1632–1636, Nov. 2016.

[5] G. Wang, H. Huang, J. Yan, Y. Cheng, and D. Fu, "An integration-implemented Newton-Raphson iterated algorithm with noise suppression for finding the solution of dynamic Sylvester equation," *IEEE Access*, vol. 8, pp. 34492–34499, 2020.

[6] L. Ding, L. Xiao, K. Zhou, Y. Lan, Y. Zhang, and J. Li, "An improved complex-valued recurrent neural network model for time-varying complex-valued Sylvester equation," *IEEE Access*, vol. 7, pp. 19291–19302, 2019.

[7] R. H. Bartels and G. W. Stewart, "Solution of the matrix equation AX+XB = C," *Commun. ACM*, vol. 15, no. 9, pp. 820–826, 1972.

[8] D. Kleinman and P. K. Rao, "Extensions to the Bartels–Stewart algorithm for linear matrix equations," *IEEE Trans. Autom. Control*, vol. AC-23, no. 1, pp. 85–87, Feb. 1978.

[9] J. Yan, X. Xiao, H. Li, J. Zhang, J. Yan, and M. Liu, "Noise-tolerant zeroing neural network for solving non-stationary Lyapunov equation," *IEEE Access*, vol. 7, pp. 41517–41524, 2019.

[10] X. Xiao, D. Fu, G. Wang, S. Liao, Y. Qi, H. Huang, and L. Jin, "Two neural dynamics approaches for computing system of time-varying nonlinear equations," *Neurocomputing*, vol. 394, no. 21, pp. 84–94, Jun. 2020.

[11] X. Xiao, C. Jiang, H. Lu, L. Jin, D. Liu, H. Huang, and Y. Pan, "A parallel computing method based on zeroing neural networks for time-varying complex-valued matrix Moore-penrose inversion," *Inf. Sci.*, vol. 524, pp. 216–228, Jul. 2020.

[12] C. Jiang, X. Xiao, D. Liu, H. Huang, H. Xiao, and H. Lu, "Nonconvex and bound constraint zeroing neural network for solving time-varying complex-valued quadratic programming problem," *IEEE Trans. Ind. Informat.*, vol. 17, no. 10, pp. 6864–6874, Oct. 2021.

[13] C. Jiang, L. Jin, and X. Xiao, "Residual-based adaptive coefficient and noise-immunity ZNN for perturbed time-dependent quadratic minimization," 2021, *arXiv:2112.01773*.

[14] T. Ogata, S. Nishide, H. Kozima, K. Komatani, and H. G. Okuno, "Intermodality mapping in robot with recurrent neural network," *Pattern Recognit. Lett.*, vol. 31, no. 12, pp. 1560–1569, Sep. 2010.

[15] S. Li, H. Cui, Y. Li, B. Liu, and Y. Lou, "Decentralized control of collaborative redundant manipulators with partial command coverage via locally connected recurrent neural networks," *Neural Comput. Appl.*, vol. 23, nos. 3–4, pp. 1051–1060, Sep. 2013.

[16] Y. Li, S. Li, and Y. Ge, "A biologically inspired solution to simultaneous localization and consistent mapping in dynamic environments," *Neurocomputing*, vol. 104, pp. 170–179, Mar. 2013.

[17] S. Li, Y. Li, and Z. Wang, "A class of finite-time dual neural networks for solving quadratic programming problems and its k-winners-take-all application," *Neural Netw.*, vol. 39, pp. 27–39, Mar. 2013.

[18] S. Li, B. Liu, and Y. Li, "Selective positive–negative feedback produces the winner-take-all competition in recurrent neural networks," *IEEE Trans. Neural Netw. Learn. Syst.*, vol. 24, no. 2, pp. 301–309, Feb. 2013.

[19] W. Duan, X. Xiao, D. Fu, J. Yan, M. Liu, J. Zhang, and L. Jin, "Neural dynamics for control of industrial agitator tank with rapid convergence and perturbations rejection," *IEEE Access*, vol. 7, pp. 102941–102950, 2019.

[20] Y. Qi, L. Jin, H. Li, Y. Li, and M. Liu, "Discrete computational neural dynamics models for solving time-dependent Sylvester equation with applications to robotics and MIMO systems," *IEEE Trans. Ind. Informat.*, vol. 16, no. 10, pp. 6231–6241, Oct. 2020.

[21] X. Yan, M. Liu, L. Jin, S. Li, B. Hu, X. Zhang, and Z. Huang, "New zeroing neural network models for solving nonstationary Sylvester equation with verifications on mobile manipulators," *IEEE Trans. Ind. Informat.*, vol. 15, no. 9, pp. 5011–5022, Sep. 2019.

[22] X. Xiao, D. Fu, G. Wang, S. Liao, Y. Qi, H. Huang, and L. Jin, "Two neural dynamics approaches for computing system of time-varying nonlinear equations," *Neurocomputing*, vol. 394, pp. 84–94, Jun. 2020.

[23] L. Jin, S. Li, H. Wang, and Z. Zhang, "Nonconvex projection activated zeroing neurodynamic models for time-varying matrix pseudoinversion with accelerated finite-time convergence," *Appl. Soft Comput.*, vol. 62, pp. 840–850, Jan. 2018.

[24] S. Liao, J. Liu, X. Xiao, D. Fu, G. Wang, and L. Jin, "Modified gradient neural networks for solving the time-varying Sylvester equation with adaptive coefficients and elimination of matrix inversion," *Neurocomputing*, vol. 379, pp. 1–11, Feb. 2020.

[25] Y. Zhang, D. Jiang, and J. Wang, "A recurrent neural network for solving Sylvester equation with time-varying coefficients," *IEEE Trans. Neural Netw.*, vol. 13, no. 5, pp. 1053–1063, Sep. 2002.

[26] S. Li, S. Chen, and B. Liu, "Accelerating a recurrent neural network to finite-time convergence for solving time-varying Sylvester equation by using a sign-bi-power activation function," *Neural Process. Lett.*, vol. 37, no. 2, pp. 189–205, 2013.

[27] Y. Shen, P. Miao, Y. Huang, and Y. Shen, "Finite-time stability and its application for solving time-varying Sylvester equation by recurrent neural network," *Neural Process. Lett.*, vol. 42, no. 3, pp. 763–784, Nov. 2015.

[28] L. Jin, Y. Zhang, and S. Li, "Integration-enhanced Zhang neural network for real-time-varying matrix inversion in the presence of various kinds of noises," *IEEE Trans. Neural Netw. Learn. Syst.*, vol. 27, no. 12, pp. 2615–2627, Dec. 2016.

[29] Z. Zhang, L. Zheng, J. Weng, Y. Mao, W. Lu, and L. Xiao, "A new varying-parameter recurrent neural-network for online solution of time-varying Sylvester equation," *IEEE Trans. Cybern.*, vol. 48, no. 11, pp. 3135–3148, Nov. 2018.

[30] Y. Zhang, K. Chen, X. Li, C. Yi, and H. Zhu, "Simulink modeling and comparison of Zhang neural networks and gradient neural networks for time-varying Lyapunov equation solving," in *Proc. 4th Int. Conf. Natural Comput.*, 2008, pp. 521–525.

[31] Y. Zhang, C. Yi, D. Guo, and J. Zheng, "Comparison on Zhang neural dynamics and gradient-based neural dynamics for online solution of nonlinear time-varying equation," *Neural Comput. Appl.*, vol. 20, no. 1, pp. 1–7, Feb. 2011.

[32] B. Ren, S. S. Ge, K. P. Tee, and T. H. Lee, "Adaptive neural control for output feedback nonlinear systems using a barrier Lyapunov function," *IEEE Trans. Neural Netw.*, vol. 21, no. 8, pp. 1339–1345, Aug. 2010.

[33] A. Lamperski and A. D. Ames, "Lyapunov theory for Zeno stability," *IEEE Trans. Autom. Control*, vol. 58, no. 1, pp. 100–112, Jan. 2013.

KUNJIAN LI received the B.E. degree in communication engineering from the Nanyang Institute of Technology, Nanyang, China, in 2020. She is currently pursuing the M.Agr. degree in agricultural engineering and information technology with the School of Electronics and Information Engineering, Guangdong Ocean University, Zhanjiang, China. Her current research interests include neural networks and computer vision.

CHENGZE JIANG (Student Member, IEEE) received the B.E. degree in software engineering from Guangdong Ocean University, Zhanjiang, China, in 2019, where he is currently pursuing the M.Agr. degree in agricultural engineering and information technology with the School of Electronics and Information Engineering. His current research interests include neural networks and computer vision.

XIUCHUN XIAO received the Ph.D. degree in communication and information system from Sun Yat-sen University, Guangzhou, China, in 2013. He is currently a Full Professor with the School of Electronics and Information Engineering, Guangdong Ocean University, Zhanjiang, China. His current research interests include artificial neural networks, image processing, and computer vision.

HAOEN HUANG received the B.E. degree in electrical engineering and automation from Guangdong Ocean University, Zhanjiang, China, in 2019, where he is currently pursuing the M.Agr. degree in agricultural engineering and information technology with the School of Electronics and Information Engineering. His current research interests include Newton algorithm, neural networks, and robotics.

YONGJIANG LI received the Ph.D. degree in cryptography from Xidian University, Xi'an, China, in 2011. He is currently an Associate Professor with the School of Mathematics and Computer Science, Guangdong Ocean University, Zhangjiang, China. His current research interests include big data and block chain application.

JINGWEN YAN received the Ph.D. degree in optics from the State Key Laboratory of Applied Optics, Changchun Institute of Fine Mechanics and Optics, Academia Sinica, Changchun, China, in 1997. He is currently a Professor with the Department of Electronic Engineering, University of Shantou, Shantou, China, where he is also the Associate Director of the Key Laboratory of Digital Signal and Image Processing of Guangdong Province and has been with the Department of Electronic Engineering, since 2006. His current research interests include SAR image processing, hyper-wavelet transforms, and compressed sensing.